

Low-loss surface modes in metamaterial waveguides

Benjamin R. Lavoie*, Patrick M. Leung, Barry C. Sanders

Institute for Quantum Information Science, University of Calgary, Alberta, T2N 1N4, Canada

Abstract

We show that waveguides with a dielectric core and a lossy metamaterial cladding (metamaterial-dielectric guide) support surface modes with lower attenuation than metal-dielectric guides. The low-loss modes are present when magnetic losses in the metamaterial are at least a factor of five below electric losses. Through a characterization of both slab and cylindrical metamaterial-dielectric guides, we find that the cylindrical geometry is a good candidate for low-intensity all-optical switches.

Keywords: Metamaterial, Waveguide, Low-loss mode

1. Introduction

Electromagnetic metamaterials are materials designed to produce an electromagnetic response that is not possible with just the constituent materials alone [1]. Within the past decade metamaterials have been of interest [2, 3], with metamaterials that operate at optical frequencies under current development [4–6]. Potential uses include cloaking devices [7], and perfect lenses [8]. Given the electromagnetic response of a metamaterial is, in principal, engineerable, there has been considerable interest in developing metamaterial waveguides [9–12]. The modes supported by metamaterial waveguides exhibit a wide range of properties with applications to improving the design of optical and near ultra-violet systems. We investigate the properties of modes in both a slab and cylindrical waveguide with a lossy metamaterial cladding and show how both waveguide geometries are able to support low-loss surface modes.

By exploiting effects that arise from surface plasmon-polaritons propagating along a single interface [13, 14], a metamaterial-dielectric waveguide is able to support low-loss surface modes. The low-loss modes in a metamaterial-dielectric waveguide display a lower attenuation than is possible for the same mode in a metal-dielectric waveguide, thereby opening up the possibility of low-loss plasmonic waveguides. The low-loss surface modes we observe are directly related to the near-zero-loss surface mode observed on a single metamaterial-dielectric interface [13]. The single-interface waveguide is used to confine the fields in order to enhance optical nonlinearity for all-optical switching on a photonic level [14]. Rather than using a single-interface waveguide for all-optical switching, we propose employing a low-loss surface mode of a cylindrical waveguide, which confines the fields in the transverse direction and could further enhance the optical nonlinearity required for all-optical control.

Energy loss, a major obstacle in the implementation of metamaterial waveguides, is present in metamaterials due to scattering and heating effects in the materials used to construct them. The artificial structure of metamaterials alters the scattering and heating effects of the materials [15]. To fully understand the properties of the modes in a metamaterial waveguide, it is crucial to include loss in the model. So far little consideration has been paid to the effects of loss [12, 16]. In order to model energy loss, we allow both the permeability and permittivity of the metamaterial to be complex-valued and frequency-dependent. For

*Corresponding author

Email addresses: brlavoie@ucalgary.ca (Benjamin R. Lavoie), pmyleung@ucalgary.ca (Patrick M. Leung), sandersb@ucalgary.ca (Barry C. Sanders)

permeability we use a Lorentz-like model that describes the behavior of metamaterials designed for optical frequencies [15], whereas the standard Drude model is used for permittivity of the metamaterial.

We compute dispersion, attenuation, and effective guide width for various modes of a cylindrical guide and, for comparison purposes, a slab guide. We show that a metamaterial-dielectric waveguide supports both surface and ordinary TM modes as well as hybrid ordinary-surface TM modes. Hybrid ordinary-surface modes are predicted for metal-dielectric parallel-plate waveguides [17], but they are only recently observed in such a guide [18]. Hybrid modes are not predicted by lossless models. We find that a metamaterial-dielectric guide is able to support hybrid modes over a much wider frequency region than is seen in metal-dielectric guides. Some modes have rapidly changing attenuation curves, with the frequency at which the change occurs depending on the structural parameters, thereby enabling a metamaterial-dielectric guide to act as a frequency filter.

2. Theory

To characterize light in a waveguide, we solve the Helmholtz equation in each region (core and cladding) for both the electric field, $\mathbf{E}(x, y, z; t)$, and the magnetic field, $\mathbf{H}(x, y, z; t)$:

$$\nabla^2 \mathbf{F}(x, y, z; \omega) = -\omega^2 \epsilon(\omega) \mu(\omega) \mathbf{F}(x, y, z; \omega), \quad (1)$$

where $\mathbf{F}(x, y, z; \omega)$ is either $\mathbf{E}(x, y, z; \omega)$ or $\mathbf{H}(x, y, z; \omega)$. We are interested in traveling plane-wave solutions, which have the form

$$\mathbf{E}(x, y, z; \omega) = \mathbf{E}(x, y) e^{i(k_z z - \omega t)} \quad (2)$$

and

$$\mathbf{H}(x, y, z; \omega) = \mathbf{H}(x, y) e^{i(k_z z - \omega t)}. \quad (3)$$

for k_z the complex propagation constant. As the permittivity and permeability of the claddings are complex functions, so too is the propagation constant $k_z := \beta + i\alpha$ with α the attenuation per unit length for a propagating field and β the propagation wavenumber. Both β and α are real and positive. A negative value for α implies the material is active (exhibits gain) whereas negative β corresponds to fields propagating in the negative z direction. Once the solutions to Eq. (1) in each region are found, we apply the appropriate boundary conditions at each interface. Applying the boundary conditions yields the dispersion relation for the waveguide, which is geometry-specific.

As we are interested in lossy waveguides, permittivity and permeability of the metamaterial must both be complex-valued and are denoted $\epsilon = \epsilon' + i\epsilon''$ and $\mu = \mu' + i\mu''$, respectively, for ϵ' , ϵ'' , μ' , and μ'' all real, and $\epsilon'' > 0$ and $\mu'' > 0$. The expressions for ϵ and μ are determined by how metamaterials are constructed [15]. A common approach used in metamaterial design for optical frequencies is to exploit the naturally occurring electric response of metals to achieve a negative permittivity and design the structure of the metamaterial to generate a magnetic response that gives a negative permeability [5].

The natural electric response of metals to an electromagnetic field is described by a frequency-dependent expression for the permittivity given by the Drude model [19]:

$$\frac{\epsilon(\omega)}{\epsilon_0} = 1 - \frac{\omega_e^2}{\omega(\omega + i\Gamma_e)}, \quad (4)$$

where ω_e is the plasma frequency of the metal and Γ_e is a damping constant. The structurally induced magnetic response of a metamaterial takes the form [15]

$$\frac{\mu(\omega)}{\mu_0} = 1 + \frac{F\omega^2}{\omega_0^2 - \omega(\omega + i\Gamma_m)}, \quad (5)$$

where F , a function of the geometry, is the magnetic oscillation strength, ω_0 is a binding frequency, and Γ_m is the damping constant for the magnetic interactions. The magnetic response is generated by resonant currents that are driven by the electromagnetic field. For parameters that are real and positive, the real

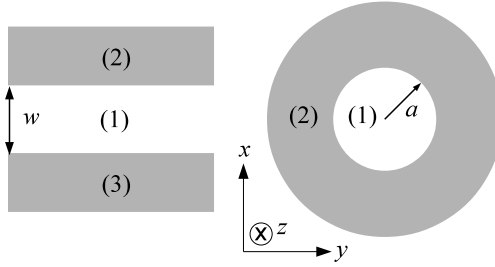


Figure 1: A diagram of the structure of the slab and cylindrical waveguides. Region (1) in both guides is the core and is a lossless dielectric, whereas regions (2), and region (3) of the slab guide are the cladding layers and are metamaterial. The width of the slab guide is w and the radius of the cylindrical guide is $a = w/2$. Fields propagate in the z direction (into the page), whereas the x and y directions are the transverse directions.

part of both Eqs. (4) and (5) can be either positive or negative whereas the imaginary parts are strictly positive.

The index of refraction of any lossy material is in general complex and given by

$$n = \pm \sqrt{\frac{\epsilon\mu}{\epsilon_0\mu_0}} = n_r + in_i, \quad (6)$$

where the sign is chosen such that $n_i \geq 0$ to ensure the material is passive (gain-free). The other case, $n_i < 0$, corresponds to a material that exhibits gain; i.e., the intensity of the fields increases as the fields propagate through the material. The choice of sign in Eq. (6) leads to the existence of frequency regions where the metamaterial displays different dispersion characteristics. At frequencies where both $\epsilon' < 0$ and $\mu' < 0$, the metamaterial behaves as a negative-index material with $n_r < 0$ and $n_i > 0$.

The frequency region where ϵ' and μ' have opposite signs (one negative and one positive) correspond to metamaterials that do not allow propagating waves. Many metals at optical frequencies act as electric plasmas and are characterized by $\epsilon' < 0$ and $\mu' > 0$; hence, for metamaterials that are similarly characterized, we use the term metallic to describe them. The metallic region is what D'Aguanno et al. call the opaque region [12]. For most frequencies in the metallic region $n_i > |n_r|$. In contrast, metamaterials with $\epsilon' > 0$ and $\mu' < 0$ are not metallic per se but would correspond to materials that display electromagnetic responses consistent with an effective magnetic plasma [3]. For frequency regions with both $\epsilon' > 0$ and $\mu' > 0$, the metamaterial simply behaves as a dielectric with a frequency-dependent refractive index.

We begin by studying the slab geometry as it has features in common with both a single interface (it has no transverse confinement) and cylindrical waveguides (it supports multiple types of modes). Additionally, the slab waveguide has been studied for various materials [20, 21], which allows us to check our methods against accepted results. The slab waveguide consists of three layers as seen in Fig. 1. The center layer is the core, and the width of the waveguide, w , is the thickness of the core. We choose the width of the slab guide to be $w = 4\pi c/\omega_e$, such that the frequency at which w is equal to the wavelength of the field is near the middle of the frequency range in which the metamaterial is metallic-like. The core is surrounded on both sides by a cladding. The cladding layers are assumed to be sufficiently thick to substantially contain the evanescent fields, as the effective width of the guide (the width of the core plus the skin depth at the interface) is typically only slightly larger than w . The permittivity and permeability of the cladding material is described by Eqs. (4) and (5) whereas they are constant in the core.

The slab guide supports two distinct classes of modes, transverse magnetic (TM) and transverse electric (TE). The TM modes have non-zero magnetic field components only in the transverse direction ($H_{z,x} = 0$) whereas the TE modes have electric field components which are non-zero only in the transverse direction ($E_{z,x} = 0$). The existence of TM surface modes in our system is partially dependent on the cladding having $\epsilon' < 0$ and $\mu' > 0$, whereas the TE modes require $\epsilon' > 0$ and $\mu' < 0$ in the cladding. As the expressions for ϵ and μ , Eqs. (4) and (5) respectively, are different, we cannot expect TE surface modes to simply be a generalization of TM surface modes. We choose to study the TM modes as the forms of the response

functions allow for the existence of TM surface modes for a large set of parameters, whereas the TE surface modes are not as robust. Applying the boundary conditions to the solutions of Eq. (1) for the TM modes leads to the dispersion relation

$$\frac{\epsilon_1}{\gamma_1} \left(\frac{\epsilon_2}{\gamma_2} + \frac{\epsilon_3}{\gamma_3} \right) = - \left(\frac{\epsilon_1^2}{\gamma_1^2} + \frac{\epsilon_2 \epsilon_3}{\gamma_2 \gamma_3} \right) \tanh \gamma_1 w, \quad (7)$$

which must be satisfied for the existence of a propagating mode [20]. Here

$$\gamma_j := \sqrt{k_z^2 - \omega^2 \epsilon_j \mu_j} \quad (8)$$

are the complex wave numbers for the transverse components of the fields for $j = 1, 2, 3$ referring to the core and two cladding layers respectively. As Eq. (7) is transcendental we solve numerically for the complex propagation constant k_z . To obtain the dispersion relation for the TE modes, simply replace any explicit appearance of ϵ_j in Eq. (7) by μ_j .

Cylindrical guides enable transverse confinement of the modes but are of interest to us for more than this reason. The cylindrical geometry is well studied in other contexts and is used in a number of applications, e.g., fiber optics. Additionally, as for the slab geometry, the dispersion relation for a guide with cylindrical geometry can be obtained analytically. The cylindrical waveguide shown in Fig. 1 consists of a dielectric cylindrical core of circular cross-section with radius a . A cladding layer, which has a frequency dependence described by Eqs. (4) and (5), surrounds the core. As with the slab geometry, the cladding layer is assumed to be arbitrarily thick.

We again assume traveling wave solutions, but we must include all components of both electric and magnetic fields. In general the modes of a cylindrical guide are not TE or TM but in-between modes that contain all of the field components and are called HE or EH [20]. The names HE and EH allude to the fact that all components of both electric and magnetic fields are non-zero. The TM and TE modes of the cylindrical guide are special cases of the general solution. Using the definitions

$$J'_m(a\kappa_1) = \left. \frac{\partial J_m(r\kappa_1)}{\partial r} \right|_{r=a}$$

and

$$K'_m(a\gamma_2) = \left. \frac{\partial K_m(r\gamma_2)}{\partial r} \right|_{r=a},$$

where J_m and K_m are the Bessel function and modified Bessel function, respectively, the dispersion relation for the cylindrical guide is [20]

$$\frac{k_z^2 m^2}{a^2 \omega^2} \left(\frac{1}{\kappa_1^2} + \frac{1}{\gamma_2^2} \right)^2 = \left(\frac{\mu_1}{\kappa_1^2} \frac{J'_m(a\kappa_1)}{J_m(a\kappa_1)} + \frac{\mu_2}{\gamma_2^2} \frac{K'_m(a\gamma_2)}{K_m(a\gamma_2)} \right) \left(\frac{\epsilon_1}{\kappa_1^2} \frac{J'_m(a\kappa_1)}{J_m(a\kappa_1)} + \frac{\epsilon_2}{\gamma_2^2} \frac{K'_m(a\gamma_2)}{K_m(a\gamma_2)} \right). \quad (9)$$

Here γ_2 is the complex wave number in the radial direction for the cladding and is given by Eq. (8), and $\kappa_1 = i\gamma_1$ is that for the core, whereas m is an integer characterizing the azimuthal symmetry. With the dispersion relations for both geometries, we are able to determine the propagation constants for the allowed modes.

3. Modes

The metamaterial-dielectric slab waveguide supports a number of TM modes with three distinct mode behaviors, namely ordinary, surface and hybrid modes. Each mode may display more than one behavior, with different behaviors supported for different frequency regions. The mode behavior is determined by the relative sizes of the wavenumber γ_1 perpendicular to the interface inside the core. To simplify the discussion we use ordinary wave, surface wave, and hybrid wave when referring to the character, or behavior, of a mode

and use the term mode or explicitly name the mode (*i.e.* TM_s) when we are talking about a specific solution to the dispersion relation.

Ordinary waves are caused by traveling electromagnetic fields inside the core reflecting from the core-cladding interface(s). The reflected fields overlap with the incident fields causing an interference effect, with constructive interference corresponding to the allowed modes. The condition for ordinary wave behavior is $\text{Im}(\gamma_1) \gg \text{Re}(\gamma_1)$, which ensures that, in the slab guide, the fields have an oscillating wave pattern in the transverse direction of the core.

Surface waves are the result of electrons at the core-cladding interface carrying energy along the waveguide. The energy from the fields is transferred to the electrons causing them to oscillate, providing a medium for energy transport. This type of coherent oscillation of electrons at a surface is called a surface polariton or surface plasmon polariton [22]. The electromagnetic field of the surface mode exponentially decays as a function of the distance from the interface. Mathematically the condition for surface waves is $\text{Re}(\gamma_1) \gg \text{Im}(\gamma_1)$, which causes the intensity to be concentrated around the interface(s) between the core and cladding and a relatively small intensity through most of the core. In slab guides only two surface wave TM modes are supported, namely symmetric (TM_s) and anti-symmetric (TM_a) according to the symmetry of the electric field component normal to the core-cladding interface.

In frequency regions where both $\text{Re}(\gamma_1)$ and $\text{Im}(\gamma_1)$ are comparable, the mode is a hybrid wave [18]. Hybrid waves can be understood as a product of two features in the transverse direction, namely an evanescent feature and an oscillatory feature. To see how the two features combine, consider the components of the electric field in the core of the the slab waveguide, which have the form

$$\begin{aligned} E &= E_0 e^{\gamma_1 x} e^{i(k_z z - \omega t)} \\ &= E_0 e^{\gamma'_1 x} e^{i\gamma''_1 x} e^{i(k_z z - \omega t)}, \end{aligned} \quad (10)$$

where E_0 is a constant, the complex wavenumber $\gamma_1 = \gamma'_1 + i\gamma''_1$, with γ'_1 and γ''_1 both real, and the terms $e^{\gamma'_1 x}$ and $e^{i\gamma''_1 x}$ represent surface wave and ordinary wave behavior, respectively. The hybrid waves are then a combination of surface waves, *i.e.*, fields being carried by electron oscillations, and ordinary waves due to fields traveling in the core and reflecting off the interfaces thereby resulting in interference effects.

For hybrid waves a substantial portion of the energy is transferred along the interfaces as well as in the core, so hybrid waves are like a combination of ordinary waves and surface waves. Hybrid waves are not seen in dielectric-dielectric guides and only for a very narrow frequency range of the TM_a mode in metal-dielectric guides, where the mode changes from a surface wave to an ordinary wave.

The metamaterial-dielectric cylindrical guide supports the same three mode types as the slab guide, though they differ slightly as the cylindrical guide has a circular symmetry. The fields of the ordinary wave TM modes in the cylindrical guide have the oscillating wave pattern of a vibrating circular membrane. The azimuthal symmetry is characterized by the integer m , which determines the number of oscillations in the fields over an angle of 2π . The fields in the cladding decay exponentially, as $\text{Re}(\gamma_2) \gg \text{Im}(\gamma_2)$. Due to the circular symmetry of the cylindrical guide it supports only one surface wave TM mode. However, the cylindrical guide supports a number of surface wave HE modes of different orders with the symmetry determined, as with the ordinary wave TM modes, by the azimuthal parameter m .

4. Characterization

With the physical nature of the three wave types supported by a metamaterial-dielectric guide understood, we now characterize the waveguides. To characterize the two guide geometries we generate plots of the effective refractive index, attenuation along the propagation direction, and effective guide width for a variety of supported modes. The following values are used for the metamaterial parameters: $\omega_e = 1.37 \times 10^{16} \text{s}^{-1}$, $\Gamma_m = \Gamma_e = 2.73 \times 10^{13} \text{s}^{-1}$, $\omega_0 = 0.2\omega_e$, $F = 0.5$ whereas the core is described by $\epsilon_1 = 1.3\epsilon_0$ and $\mu_1 = \mu_0$.

We characterize the slab geometry first, and, to provide a basis for comparison, we also include in some plots the results for a metal-dielectric waveguide. Also, we assume the slab guide is symmetric, meaning all of the parameters are identical for both cladding layers. A large peak occurs at $\omega = 0.2\omega_e$ in the plots of

Table 1: The different regions of the metamaterial, determined by the parameter choice, are identified by the sign of the real part of both the permittivity and the permeability.

Frequency Range	Sign of ϵ' , μ'	Property
$1 < \omega/\omega_e$	$\epsilon' > 0$, $\mu' > 0$	Dielectric-like
$0.3 \lesssim \omega/\omega_e < 1$	$\epsilon' < 0$, $\mu' > 0$	Metal-like
$0.2 \lesssim \omega/\omega_e \lesssim 0.3$	$\epsilon' < 0$, $\mu' < 0$	Negative-index media
$\omega/\omega_e \lesssim 0.2$	$\epsilon' < 0$, $\mu' > 0$	Metal-like

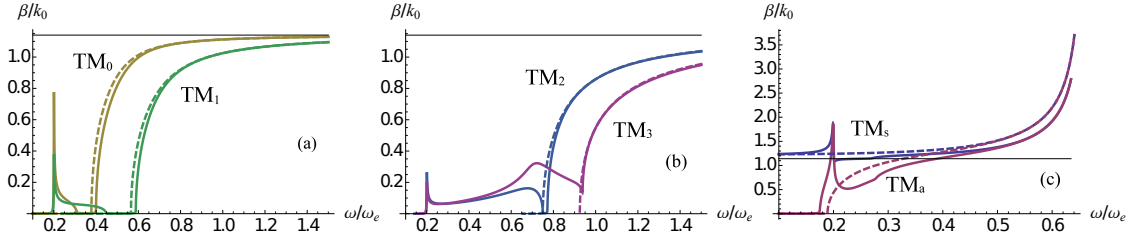


Figure 2: Effective refractive index for (a) the TM_0 and TM_1 , (b) the TM_2 and TM_3 , and (c) the TM_s and TM_a modes of the slab guide. The solid lines are for the modes of the metamaterial-dielectric guide, and the dashed lines are for the modes of the metal-dielectric guide. The thin horizontal line in (a) and in (b) is the refractive index of the core.

effective refractive index and is due to a resonance in the expression for the permeability. The parameters we use to describe the metal are the same as for the metamaterial, with the exception that $\mu_{2,3} = \mu_0$.

Frequency regions with differing refractive index characteristics for the metamaterial can be identified (Table 1) when the above parameters are used along with Eqs. (4) and (5). Above ω_e the metamaterial behaves as a lossy dielectric with both $\epsilon' > 0$ and $\mu' > 0$. There are two metallic regions, one for $0.3\omega_e \lesssim \omega < \omega_e$ and one for $\omega \lesssim 0.2\omega_e$. We say metallic because the regions are characterized by $\epsilon' < 0$ and $\mu' > 0$, which is typical for metals at optical frequencies but not seen in dielectrics. In the frequency range $0.2\omega_e \lesssim \omega \lesssim 0.3\omega_e$ the metamaterial has a negative-index.

All guided modes in a waveguide experience an effective refractive index along the propagation direction. The effective refractive index of a waveguide is related to the propagation constant, β , by the relation $n_{\text{eff}} = \beta/k_0$ with $k_0 = \omega/c$ the free-space wave number, and c is the speed of light in vacuum. As an example of n_{eff} for ordinary waves in the slab guide, the effective refractive index of the modes TM_0 and TM_1 is plotted versus frequency in Fig. 2(a). The TM_0 mode is an ordinary wave for frequencies above $\omega \approx 0.3\omega_e$, and the TM_1 mode is an ordinary wave above $\omega \approx 0.45\omega_e$. Below these frequencies the two modes show hybrid wave behavior, which is discussed later. The effective refractive index of ordinary waves in a metamaterial-dielectric guide is very similar to that of a dielectric-dielectric guide, increasing with the frequency of the wave and bound from above by the refractive index of the core, $n_{\text{core}} = \frac{1}{c}\sqrt{\epsilon_1\mu_1}$.

Modes with surface wave behavior exist in metal-dielectric guides as well as in metamaterial-dielectric guides. The requirement of ϵ' or μ' to have opposite signs on either side of the interface means surface modes are not possible in dielectric-dielectric guides. Only two modes in the slab guide show surface wave characteristics, TM_s and TM_a . The effective refractive index of surface waves in a metamaterial-dielectric guide behaves as in a metal-dielectric guide, increasing with the frequency, and is plotted for the slab-guide modes TM_s and TM_a in Fig. 2(c). The modes display surface wave behavior at frequencies such that $n_{\text{eff}} > n_{\text{core}}$, and the TM_a mode displays ordinary wave behavior for frequencies below $0.2\omega_e$ and for $0.3\omega_e \lesssim \omega \lesssim 0.4\omega_e$.

Hybrid waves often exhibit anomalous dispersion (decreasing n_{eff} with increasing frequency). We have already seen hybrid mode behavior in Fig. 2(a), where it is present at lower frequencies than the ordinary wave of the same mode. There are also regions of hybrid wave behavior in the TM_s and TM_a modes, shown

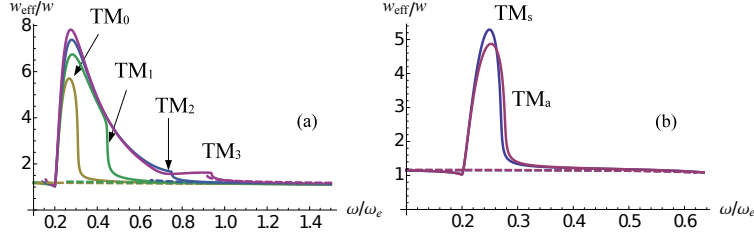


Figure 3: Effective guide width for (a) the TM_0 to TM_3 , and (b) the TM_s and TM_a modes of the slab guide. Solid lines are for the metamaterial-dielectric guide, and dashed lines are for the metal-dielectric guide.

in Fig. 2(c), which occur within the negative index region ($0.2\omega_e \lesssim \omega \lesssim 0.3\omega_e$) for both modes and in a narrow region around $0.4\omega_e$ for the TM_a mode.

Figure 2(b) shows the effective refractive index for the TM_2 and TM_3 modes of the metamaterial-dielectric slab waveguide. The hybrid wave behavior occurs for $\omega \lesssim 0.75\omega_e$ in the TM_2 mode and $\omega \lesssim 0.95\omega_e$ in the TM_3 mode. Both modes have regions of anomalous dispersion with a particularly large frequency region of anomalous dispersion in the TM_3 mode.

The effective guide width of a waveguide, w_{eff} , is the nominal width, w , plus the skin-depth at each interface, where $w_{\text{eff}} = w + 1/\text{Re}(\gamma_2) + 1/\text{Re}(\gamma_3)$ for the slab guide. Ordinary and surface waves in a metamaterial-dielectric guide have an effective width that is only slightly larger than the nominal width; this is consistent with ordinary and surface waves of a metal guide. Hybrid waves, however, display an increased effective width when compared to the ordinary and surface waves. Figures 3(a) and 3(b) are plots of the relative effective width w_{eff}/w and show the large effective width of the hybrid waves. The largest effective width for each mode is seen in the negative index region, where all modes are hybrid waves. Significantly increased effective width is a feature unique to metamaterial guides. The effective width of metal-dielectric and dielectric-dielectric guides does not have such a large variation.

A large effective width means the intensity of the mode decays slowly in the cladding, meaning a significant fraction of the energy is carried outside the core. As the cladding dissipates energy, there is a connection between large effective width and large losses. The surface waves, however, can have a small effective width even when there is a large fraction of the total energy in the cladding, which is due to the fact that the energy of a surface mode is concentrated around the interface with almost no energy in the center of the core. Thus, even when there is a rapid decay of the intensity in the cladding, there can be an equally rapid decay away from the interface in the core. The effect, then, is a relatively even distribution of energy about the interface and a small effective width.

The attenuation of a mode in a waveguide is a measure of how quickly the intensity of the mode decreases as a function of the distance travelled. The imaginary part of k_z is called the attenuation constant, denoted as α , and defines the rate per unit length at which the amplitudes of the fields decrease. All of the mode types in the metamaterial guide show some amount of attenuation, with some wave types having more than others.

Hybrid waves have the largest attenuation, which is partly due to their large effective width. The attenuation of the TM_2 and TM_3 modes of the slab guide is seen in Fig. 4(a). The regions of large attenuation occur where the modes display hybrid wave behavior. Hybrid waves also have larger attenuation than surface waves in the same mode, though the difference is much less pronounced. The attenuation of the TM_s and TM_a modes is shown in Fig. 4(b).

At frequencies where the mode displays hybrid wave behavior the attenuation is considerably larger than for either ordinary wave or surface wave behavior. The exception is the TM_a mode for $\omega \lesssim 0.2\omega_e$ where it is an ordinary wave. Here the attenuation is large also but is consistent with the TM_a mode in the metal guide (see the dashed line in Fig. 4(b)), which is also an ordinary wave at low frequencies. The attenuation of both ordinary and hybrid waves decreases as the frequency increases, whereas the attenuation of surface waves generally increases with increasing frequency.

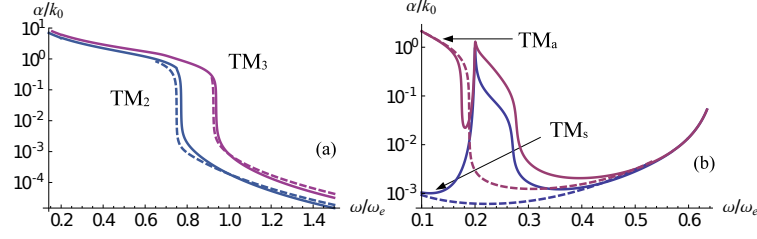


Figure 4: Attenuation for (a) the TM_2 and TM_3 , and (b) the TM_s and TM_a modes of the slab guide. Solid lines are for the metamaterial-dielectric guide, and dashed lines are for the metal-dielectric guide.

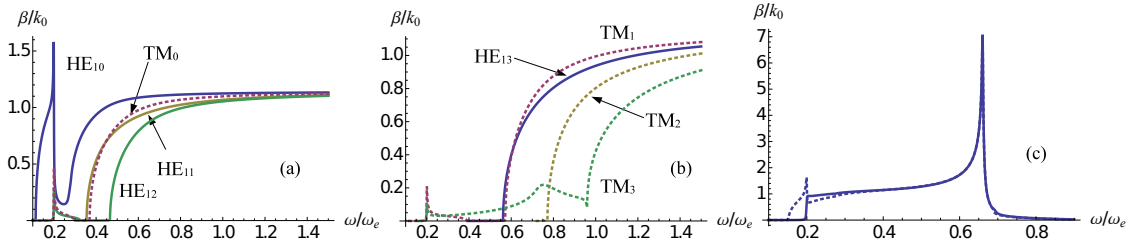


Figure 5: Effective refractive index for (a) the HE_{10} to HE_{12} , and TM_0 , (b) the HE_{13} , and TM_1 to TM_3 , and (c) the HE_{1s} and TM_s modes of the metamaterial-dielectric cylindrical guide. The solid lines indicate HE modes and the dotted lines indicate TM modes.

Ordinary waves in a cylindrical guide display similar dispersion characteristics to those in a slab guide, including the appearance of hybrid waves at lower frequencies. Figure 5(a) shows n_{eff} for the four modes HE_{10} , HE_{11} , HE_{12} , and TM_0 of the metamaterial cylindrical guide. The modes are ordinary waves for the frequencies $\omega \gtrsim 0.25\omega_e$ for the HE_{10} mode and $\omega \gtrsim 0.3\omega_e$ for the HE_{11} , HE_{12} and TM_0 modes. Below these frequencies the modes are hybrid waves, except for the HE_{11} mode, which has a cut-off at $\omega \sim 0.3\omega_e$ and does not display hybrid wave behavior.

Modes with surface wave behavior are supported by the metamaterial-dielectric cylindrical guide as well. The cylindrical guide supports a number of modes with surface wave behavior (one TM and the rest HE), all of different orders (number of oscillations in the electric field over an angle of 2π). The effective refractive index of the two lowest-order surface modes, TM_s and HE_{1s} , supported by the cylindrical guide is shown in Fig. 5(c).

Hybrid waves occur in cylindrical guides as well though not for every mode (see Fig. 5(b)). Specifically the HE_{13} and TM_2 modes of the cylindrical guide, along with the HE_{11} mode mentioned earlier, do not display hybrid wave behavior for our choice of parameters, whereas the TM_1 mode is a hybrid wave for $\omega \lesssim 0.4\omega_e$ and the TM_3 mode is a hybrid wave for $\omega \lesssim 0.95\omega_e$.

The effective widths of the modes supported by the metamaterial-dielectric cylindrical guide show similar characteristics to the effective widths of the modes in a metamaterial-dielectric slab guide. Figure 6(a) shows the effective width of the four modes HE_{13} , TM_1 , TM_2 , and TM_3 of the cylindrical guide, and Fig. 6(b) shows the width for the HE_{1s} and TM_s modes. The effective widths of the ordinary and surface waves are only slightly larger than the nominal width of the guide, whereas the effective widths of the hybrid waves are large, when compared to the nominal guide width and the effective widths of the other wave types. The large effective width of the HE_{1s} and TM_s modes at higher frequencies is due to the fact that the value of n_{eff} for the modes is becoming similar to the refractive index of the metamaterial, thus lessening the contrast between the core and cladding, allowing the fields to penetrate further into the cladding. The HE_{1s} and TM_s modes are actually ordinary waves for $\omega \gtrsim 0.65\omega_e$, not hybrid waves.

As with the effective widths, the attenuation of the modes of the metamaterial-dielectric cylindrical guide

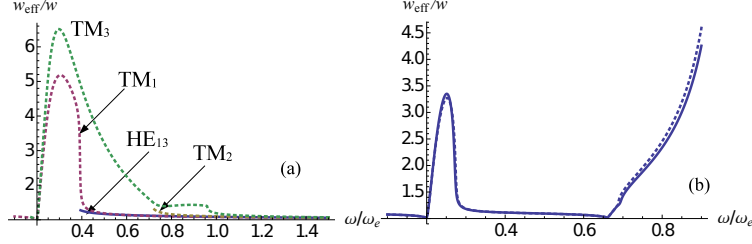


Figure 6: Effective guide width for (a) the HE_{13} mode, and TM_1 to TM_3 , and (b) the HE_{1s} and TM_s modes of the metamaterial-dielectric cylindrical guide. The solid lines indicate HE modes and the dotted lines indicate TM modes.

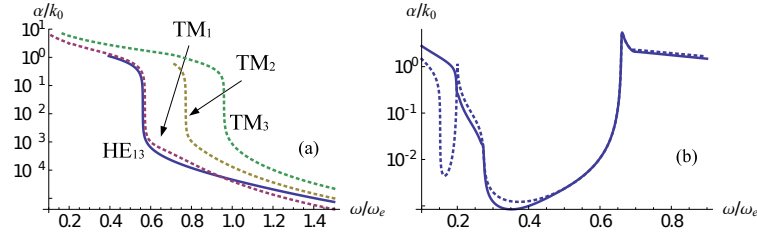


Figure 7: Attenuation for (a) the HE_{13} and TM_1 to TM_3 , and (b) the HE_{1s} and TM_s modes of the metamaterial-dielectric cylindrical guide. The solid lines indicate HE modes and the dotted lines indicate TM modes.

is similar to that of the slab guide. The attenuation for the HE_{13} , TM_1 , TM_2 , and TM_3 modes is shown in Fig. 7(a). In frequency regions of hybrid wave behavior the modes have large attenuation compared to where they are ordinary waves. The same trend of decreasing attenuation with increasing frequency is also present. The TM_s and HE_{1s} modes of the cylindrical guide, shown in Fig. 7(b), have attenuation characteristics similar to the TM_a mode of the slab guide.

We now have a better understanding of how metamaterial-dielectric waveguides behave when the effect of absorption is considered. The subject of possible implications and implementations of such waveguides can now be approached.

5. Discussion: Low-loss surface modes

In a metamaterial-dielectric guide, attenuation of ordinary and surface waves is much less than for hybrid waves but is still comparable to attenuation in metal-dielectric waveguides. With current metamaterial technology, losses due to atomic interaction with the magnetic field are significant [6, 15]. Previous results for superconducting metamaterials [23] show magnetic losses could be reduced, thereby opening up the possibility of low-loss metamaterial-dielectric waveguides. By reducing the magnetic loss, we take advantage of effects discovered by Kamli, Moiseev and Sanders [13, 14] to reduce the attenuation of metamaterial-dielectric waveguides.

The losses associated with the magnetic interaction are parameterized by Γ_m . We choose $\Gamma_m = \Gamma_e/1000$ to generate the plots, in order to emphasize the low-loss region, but the magnetic losses need only be a factor of five below the electric losses (i.e. $\Gamma_m = \Gamma_e/5$) for the metamaterial guide to have less attenuation than a metal guide. Figure 8(a) shows a comparison of the TM_s modes for the metamaterial slab guide ($\Gamma_m = \Gamma_e = 2.73 \times 10^{13} \text{s}^{-1}$), the metal slab guide ($\Gamma_m = 0$), and the metamaterial slab guide with reduced magnetic losses ($\Gamma_m = \Gamma_e/1000$). The attenuation dip seen in metamaterial-dielectric waveguides is related to that seen for surface waves on a single metamaterial-dielectric interface [13, 14]. The solution for a single interface, as well as the attenuation dip, is recovered from the metamaterial guides in the limit of large guide width. Similarly, the HE_{1s} surface mode of the cylindrical guide has reduced attenuation for $\Gamma_m \ll \Gamma_e$. In

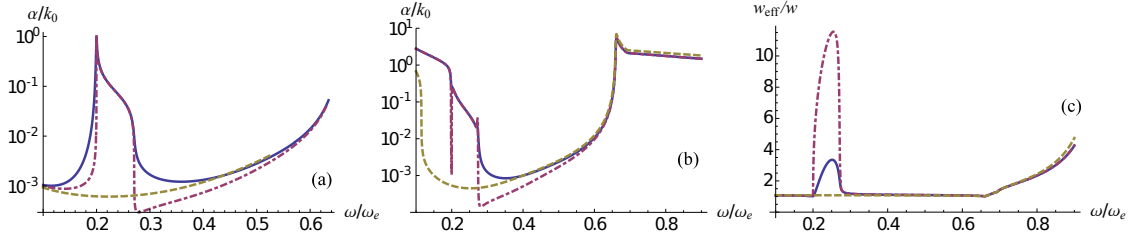


Figure 8: Attenuation for (a) the TM_s mode of the slab guide and (b) the HE_{1s} mode of the cylindrical guide, and (c) the effective width of the HE_{1s} mode of the cylindrical guide. The solid line is for the metamaterial-dielectric guide, the dashed line is for the metal-dielectric guide and the dot-dashed line is for a metamaterial-dielectric guide with $\Gamma_m = \Gamma_e/1000$ for the metamaterial.

Fig. 8(b), the attenuation of the HE_{1s} mode in the metamaterial cylindrical guide at $\omega = 0.3\omega_e$ is 0.36 times that of the HE_{1s} mode in the metal cylindrical guide.

Reducing the value of Γ_e , which parameterizes loss due to atomic interactions with the electric field, also has the effect of reducing the total attenuation of the TM and HE modes in a metamaterial-dielectric waveguide. However, reducing Γ_e for a metal-dielectric waveguide also reduces the attenuation of its TM and HE modes. Thus for a metamaterial-dielectric waveguide, reducing Γ_e alone does not yield any benefit over a similar reduction for a metal-dielectric waveguide. The benefit is in combining the reduced Γ_e with a reduced Γ_m to compound the two effects, which significantly reduces attenuation in metamaterial-dielectric waveguides.

All-optical control of low-intensity pulses has two major requirements, namely low attenuation and strong transverse field confinement for large cross-phase modulation. The cylindrical metamaterial-dielectric guide must meet the two requirements simultaneously to suffice for all-optical switching. The first requirement, low attenuation, allows a low-intensity pulse to pass through the guide without being lost. By extending the results of Kamli, Moiseev and Sanders, we have shown cylindrical metamaterial-dielectric waveguides can have reduced losses under the right conditions, i.e., reduced magnetic losses.

The second requirement is strong confinement of the field in the transverse direction (normal to the core/cladding interface). Strong confinement allows the pulse to be confined to a smaller volume, thus increasing the local field intensity and enhancing the nonlinear response. As the low-loss modes of the cylindrical guide are surface waves, which are inherently confined to the interface along which they propagate, the metamaterial-dielectric cylindrical waveguide is a good candidate for enhancing cross-phase modulation between low-intensity pulses.

Metamaterial-dielectric waveguides support modes with three distinct regimes, ordinary, surface, and hybrid ordinary-surface waves. The existence of the hybrid wave regime is a direct result of the waveguide dissipating energy. Models for metamaterial waveguides that do not dissipate energy (lossless), do not predict hybrid modes [9, 10] due to the fact that the wavenumbers in the lossless model are allowed to be either real or imaginary, but not complex. Thus, the supported modes are either surface or ordinary waves, respectively. Modelling the waveguide with a dissipative material allows the wavenumbers to be complex, meaning the modes can have characteristics of both surface and ordinary waves. Hybrid waves in metamaterial-dielectric guides are much more robust than those in a metal-dielectric guide; i.e., they are supported for a much broader frequency range. The wider frequency range may make observing hybrid waves in practice easier for metamaterial guides than for metal guides.

Modes with hybrid wave behavior also have large attenuation relative to the other supported wave types. One possible use of hybrid modes is frequency filtering to remove unwanted frequencies from pulses. Pulses with frequencies outside of the hybrid wave region are allowed to propagate further, either as an ordinary wave or as a surface wave depending on the mode. Any pulse with frequencies that fall in the region of large attenuation propagate as a hybrid wave and are quickly extinguished.

6. Summary

Our results show that reducing the energy loss associated with the magnetic interactions reduces the attenuation of the surface modes in metamaterial-dielectric waveguides. For $\Gamma_m \leq \Gamma_e/5$ the attenuation is reduced below even that for a metal-dielectric guide within a certain frequency range, despite the metal and metamaterials having identical expressions for the permittivity. When $\Gamma_m = \Gamma_e/1000$, the attenuation of the HE_{1s} mode in the metamaterial cylindrical guide at $\omega = 0.3\omega_e$ is about one-third that of the HE_{1s} mode in the metal cylindrical guide. With the use of superconducting metamaterials, or some other means of reducing Γ_m , it is possible, in principle, to construct metamaterial-dielectric waveguide devices with very low losses. With the capability of transverse confinement while supporting low loss modes, the metamaterial cylindrical guide is a good candidate for enhancing cross-phase modulation and ultimately all-optical control of low-intensity signals.

We have examined the modal properties of a slab and cylindrical metamaterial-dielectric waveguide using a model that includes energy loss. We have shown that the modes of metamaterial-dielectric waveguides support three distinct regimes, namely ordinary, surface and hybrid, with hybrid modes being a feature unique to models that include energy loss. Ordinary and surface modes are well known and have been studied previously. Hybrid waves, however, have not been previously examined for metamaterial-dielectric waveguides. Furthermore, though the existence of a hybrid mode was predicted for metal-dielectric parallel plate waveguides some time ago [17], they have only recently been observed [18] in an experimental setting.

Ordinary waves have the bulk of their energy distributed throughout the core and are the result of internal reflections and interference effects. Surface waves, on the other hand, have their energy concentrated at the interface(s) of the guide, which is due to the fact that the energy is being transported along the guide through the oscillations of surface electrons. Hybrid waves, as their name suggests, show a combination of the two mechanisms and thus their respective energy distributions.

Hybrid waves typically have a large effective width when compared to the other mode types, which implies a large amount of energy is in the cladding. When the energy of a mode is carried in a cladding that dissipates energy, the result is attenuation of the field. Our model allows for a lossy cladding so the increased amount of energy in the cladding for hybrid modes is consistent with the increased attenuation. Within the negative-index frequency range of the metamaterial, all of the modes of the waveguide are hybrid waves and display the associated large attenuation and increased effective guide width.

The sharp change seen in the attenuation curves could be advantageous as a frequency filter. A pulse propagating through a metamaterial guide would have the frequency components in the high-attenuation regions removed through energy dissipation, while the remainder of the pulse continues to propagate. The frequencies at which the attenuation change occurs may be selected through the design of the metamaterial.

Acknowledgements

We appreciate valuable discussions with S. A. Moiseev and A. Kamli and financial support from AITF and NSERC. BCS is partially supported by a CIFAR Fellowship.

References

- [1] G. V. Eleftheriades, K. G. Balmain (Eds.), *Negative-Refractive Metamaterials*, John Wiley & Sons, Inc., Hoboken, 2005.
- [2] A. D. Boardman, N. King, L. Velasco, Negative refraction in perspective, *Electromagnetics* 25 (2005) 365–389.
- [3] S. A. Ramakrishna, Physics of negative index materials, *Rep. Prog. Phys.* 68 (2005) 449–521.
- [4] V. M. Shalaev, Optical negative-index materials, *Nature Photon.* 1 (2007) 41–48.
- [5] A. Boltasseva, V. M. Shalaev, Fabrication of optical negative-index metamaterials: Recent advances and outlook, *Metamaterials* 2 (2008) 1–17.
- [6] S. Xiao, U. K. Chettier, A. V. Kildishev, V. P. Drachev, V. M. Shalaev, Yellow-light negative-index metamaterials, *Opt. Lett.* 34 (2009) 3478–3480.
- [7] W. Cai, U. K. Chettier, A. V. Kildishev, V. M. Shalaev, Optical cloaking with metamaterials, *Nature Photon.* 1 (2007) 224 – 227.
- [8] J. B. Pendry, Negative refraction makes a perfect lens, *Phys. Rev. Lett.* 85 (2000) 3966–3969.

- [9] I. V. Shadrivov, A. A. Sukhorukov, Y. S. Kivshar, Guided modes in negative-refractive-index waveguides, *Phys. Rev. E*. 67 (2003) 057602.
- [10] D.-K. Qing, G. Chen, Nanoscale optical waveguides with negative dielectric cladding, *Phys. Rev. B* 71 (2005) 153107.
- [11] J. He, Y. Jin, Z. Hong, S. He, Slow light in a dielectric waveguide with negative-refractive-index photonic crystal cladding, *Opt. Express* 16 (2008) 11077–11082.
- [12] G. D'Aguanno, N. Mattiucci, M. Scalora, M. J. Bloemer, TE and TM guided modes in an air waveguide with negative-index-material cladding, *Phys. Rev. E* 71 (2005) 046603.
- [13] A. Kamli, S. A. Moiseev, B. C. Sanders, Coherent control of low loss surface polaritons, *Phys. Rev. Lett.* 101 (2008) 263601.
- [14] S. A. Moiseev, A. A. Kamli, B. C. Sanders, Low-loss nonlinear polaritonics, *Phys. Rev. A* 81 (2010) 033839.
- [15] R. S. Penciu, M. Kafesaki, Th. Koschny, E. N. Economou, C. M. Soukoulis, Magnetic response of nanoscale left-handed metamaterials, *Phys. Rev. B*. 81 (2010) 235111.
- [16] J. He, S. He, Slow propagation of electromagnetic waves in a dielectric slab waveguide with a left-handed material substrate, *IEEE Microw. Wireless Compon. Lett.* 16 (2005) 96–98.
- [17] H. M. Barlow, High-frequency wave propagation between parallel surfaces very close together, *J. Phys. D: Appl. Phys.* 6 (1973) 929–935.
- [18] J. Liu, R. Mendis, D. M. Mettlem, The transition from a TEM-like mode to a plasmonic mode in parallel-plate waveguides, *Appl. Phys. Lett.* 98 (2011) 231113.
- [19] B. E. Sernelius, *Surface Modes in Physics*, Wiley-VCH, Berlin, 2001.
- [20] C. Yeh, F. Shimabukuro, *The Essence of Dielectric Waveguides*, Springer Science+Business Media, New York, NY, 2008.
- [21] I. P. Kaminow, W. L. Mammel, H. P. Webber, Metal-clad optical waveguides: Analytical and experimental study, *Appl. Opt.* 13 (1974) 396–405.
- [22] J. Nkoma, R. Loudon, D. R. Tilley, Elementary properties of surface polaritons, *J. Phys. C: Solid State Phys.* 4 (1974) 3547–3559.
- [23] M. C. Ricci, S. M. Anlage, Single superconducting split-ring resonator electrodynamics, *Appl. Phys. Lett.* 88 (2006) 264102.